Langmuir

Article

pubs.acs.org/Langmuir

Studying Light Propagation in Self-Assembled Hybrid Photonic–Plasmonic Crystals by Fourier Microscopy

J. F. Galisteo-López,* M. López-García, A. Blanco,* and C. López

Instituto de Ciencia de Materiales de Madrid (ICMM-CSIC), C/Sor Juana Inés de la Cruz 3, 28049 Madrid, Spain

ABSTRACT: Hybrid metallodielectric systems where dielectric components are combined with metals supporting surface plasmons are able to spatially redistribute the electromagnetic field intensity within its volume through hybrid photonic–plasmonic modes. While most of the work done recently in this kind of systems has been focused on the way such redistribution takes place and how light couples to or is emitted from such samples, the way light propagation takes place has not been studied in depth. Here we consider light propagation in hybrid systems fabricated by self-assembly methods measuring their equifrequency surfaces both in reflection and emission configurations. Comparing spectroscopic measurements with equifrequency surfaces provides a deeper insight into the way light propagates in these structures, showing the possibilities they may present for several applications.

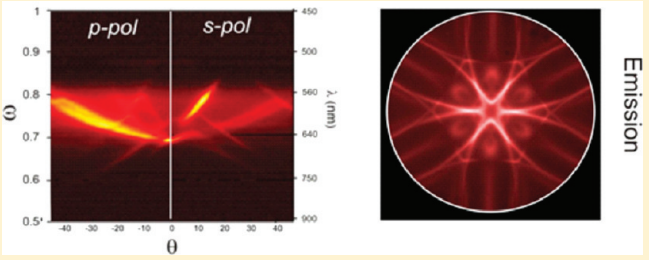

INTRODUCTION

There is a current interest in the combination of dielectric nanophotonic elements with metallic ones supporting surface plasmon polaritons (SPP) in the shape of hybrid photonic–plasmonic systems as a means to develop structures that can outperform the individual components.[1,2] Through the appropriate design of the structure, one can, for instance, achieve large electromagnetic (EM) field enhancements in volumes of subwavelength dimensions reducing the losses characteristic of plasmonic systems. Among the many routes explored to fabricate such hybrid structures, the combination of photonic systems made by self-assembly of colloidal particles[3] in combination with metals[4] has been actively explored, particularly in the form of two-dimensional (2D) arrays of dielectric submicrometer spheres on metallic substrates. Using the latter approach, several studies have demonstrated the existence of hybrid photonic–plasmonic modes where the EM field intensity undergoes a strong spatial redistribution.[5−8] Such redistribution can be used as a means to modulate the spontaneous emission of internal light sources,[6] develop chemical sensors,[7] or improve the efficiency of photovoltaic devices.[8]

In this kind of structure, the EM field is distributed in the form of hybrid modes which are extended in the plane of periodicity. Such modes have a leaky character and can therefore be coupled to impinging light coming from out of the plane of periodicity, similar to 2D photonic crystal (PC) slabs.[9] Hence, most of the optical characterization of these systems has been done in the form of reflectance and transmittance spectroscopy which provide information on the angular and spectral features of the different modes, that is, their dispersion relation. Such measurements, though highly valuable, fail to provide information on the way light propagates in the plane of periodicity. This information can be retrieved, for instance, by using light traveling parallel to the plane of periodicity and observing how it propagates as has been demonstrated in 2D PC[10] or by obtaining the equifrequency surface (EFS)[11] at any given frequency. Both means are equivalent and as a matter of fact, and EFSs have been retrieved from in-plane propagation measurements.[12]

An EFS is in essence the loci of all allowed wave vectors k in the plane of periodicity for a frequency ω and provides information regarding the refraction of light as it propagates in the plane of periodicity. EFS being such a useful tool to understand light propagation in periodically nanostructured materials, several approaches have been explored in order to study them. For the case of 2D PC, besides direct visualization methods such as the ones mentioned above or collecting light emission in the far field,[13] other techniques have been employed such as phase-sensitive near field microscopy[14] or imaging the Fourier or k-space collecting scattered light.[15] The latter has been recently extended to the study of EFS in purely plasmonic 1D and 2D period arrays in a transmission configuration,[16] showing how the refractive properties of periodic dielectric structures can also be found in their metallic counterparts. Also recently, the interest in EFS has been extended to hybrid metallodielectric structures, where light scattering due to the presence of unintentional defects was used to image EM modes in the far field.[17]

In this paper, we study how light propagates in the plane of periodicity of hybrid metallodielectric structures fabricated by self-assembly methods. First we consider two fabrication

Special Issue: Colloidal Nanoplasmonics

Received: January 31, 2012
Revised: April 2, 2012
Published: April 2, 2012

   dx.doi.org/10.1021/la300448y | *Langmuir* 2012, 28, 9174–9179

methods, and explore the microstructure of the fabricated samples from the point of view of their crystallinity, seeking the one which presents a monodomain structure and is therefore better suited for studying EFS. Next we optically characterize their optical response by Fourier microscopy obtaining both spectroscopic measurements as well as EFS. The latter characterization is performed in both reflection and emission configurations, obtaining in this way a complete picture on how light propagates in this kind of hybrid system.

EXPERIMENTAL SECTION

Sample Fabrication. The samples under study consist of hexagonal close packed monolayers of polystyrene spheres grown on thin (60 nm) silver films deposited on silicon substrates. The metallic films were coated by sputtering with a 6 nm film of Si_3N_4 in order to avoid oxidation of the silver surface after exposure to air or water. The surface roughness of the final substrate was below 1 nm over a cm^2 area as evidenced by atomic force microscopy inspection (not shown). Finally the substrates were hydrophilized prior to monolayer deposition (see below) by exposure to a temperature controlled oxygen plasma working at room temperature and 0.4 mbar for 30 s. Highly monodisperse (3%) polystyrene spheres with a diameter of ϕ = 520 nm were used as provided by the manufacturer (Thermo Scientific). The spheres are homogeneously doped with Rhodamine 6G, allowing the study of the spontaneous emission of internal light sources.

In order to fabricate the ordered arrays, two methods were tested: the vertical deposition and the wedge shaped cell method. Both methods are thoroughly described in refs 18 and 19, respectively. In what follows, we will only provide those parameters which led to the highest quality samples for each case in terms of sample size, homogeneity, and crystalline quality, relevant for their optical response which is of interest for us. In both cases, samples were grown in a temperature/humidity controlled chamber.

For samples grown by the vertical deposition method, the substrates were placed in 20 mL glass vials containing 5 mL of an aqueous colloidal suspension. In order to obtain a monolayer rather than a three-dimensional array (i.e., an artificial opal), the sphere concentration was lowered to 0.08% wt. The temperature and humidity were set in the growth chamber to 45 °C and 30%, respectively. Finally, the angle at which the substrate is placed in the vial, which influences the meniscus shape and thus the sample quality,[20] was 20° with respect to the vertical direction. The obtained samples presented regions of several mm^2 which appeared uniformly colored to the naked eye. In order to better appreciate the crystalline quality of the samples, a closer inspection was done under the scanning electron microscope (SEM). Figure 1 shows a typical SEM image with spatial Fourier transforms (FT) of two adjoining regions of ~20 μm^2. From the FT images, which present the expected hexagonal pattern corresponding to a close packed lattice, it is clear that although observing the whole image the sample seems to consist of a single domain and it is made of smaller domains rotated with respect to each other. This microstructure can hamper the interpretation of the optical response, since what we are interested in is the full spectral and angular response of the samples, and the presence of differently oriented domains will overlap several angular responses making their interpretation a nontrivial task. Hence, an alternative growth method was sought. Finally, it can be seen that although some random vacancies and dislocations are present, the overall lattice is close packed.

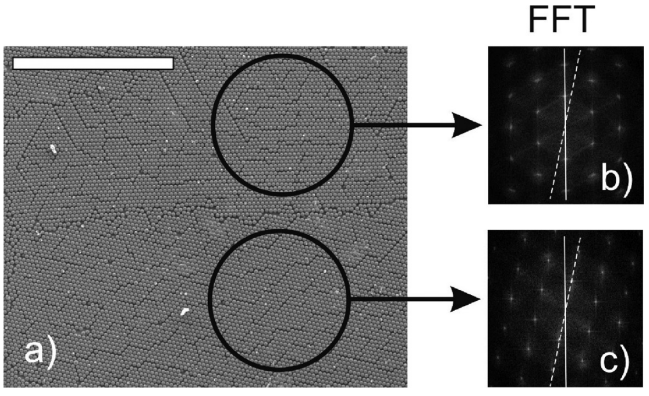

Figure 1. (a) SEM image of a self-assembled hybrid structure grown on a silver substrate by the vertical deposition method using PS spheres with ϕ = 520 nm diameter. Scale bar corresponds to 20 μm. (b,c) Calculated FT images of the regions surrounded by black circles.

In order to solve the previous structural issues, we employed the recently proposed method of the wedge shaped cell[19] for which single monolayer domains extending over cm^2 have been reported. Here a 100 μL colloidal suspension with a larger concentration (1% wt) was placed in a wedge cell formed by the metal substrate and a glass slide at an angle of 2°. The temperature and humidity in this case were set to 20 °C and 90%, respectively. Figure 2 shows an SEM image of a typical sample and its FT, showing that the hexagonal order remains for regions as large as 100 μm, the latter being the diameter of the probe beam. Hence, we are sure that the probed region consists of a single domain and spurious effects on the optical response coming from probing several domains are avoided. A number of defects,[21] that is, concentration of vacancies and lattice dislocations among others, as in the previous method are still present and known to introduce some diffuse scattering. These are the samples whose optical response will be studied throughout the present work.

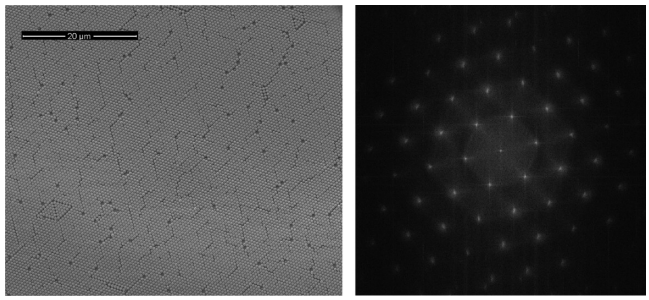

Figure 2. (Left) SEM image of a sample similar to the one in Figure 1 only that grown by the wedged cell method. (Right) FT image of the SEM image.

Optical Characterization. The optical response was measured employing a previously described experimental setup.[22] In brief, an inverted optical microscope with a high numerical aperture (Zeiss EC Plan-Neofluar, NA = 0.75, 40×) objective was used to image the sample. An enlarged image of the back focal plane of the objective was projected outside the microscope and diverted into two arms. An arm is imaged with a CCD camera in front of which a tunable optical interference filter (Semrock TBP01-700/13-25x36) was placed in order to obtain EFS at a given wavelength in the 610−700 nm range ±10 nm. Additionally, a narrow spectral filter (Semrock Maxline) was used to acquire EFS with better resolution at 632.8 ±2.5 nm.

The other arm projects an enlarged (d = 8 mm) image which is scanned along its diameter with a stepper motor driven optical fiber coupled to a spectrometer (Ocean USB 200+). In this way, spectra can be collected as a function of angle from normal incidence to the maximum angle collected by the microscope objective (48°). Illumination of the sample is performed through the same collection objective either with white light for reflection measurements or with a monochromatic diode laser (485 nm) for spontaneous emission measurements. Experimental spectra were collected for s and p polarization (corresponding to light having its electric field oscillating normal to or within the plane of reflection, fiber scan line, respectively) by placing a properly oriented polarizer before the detector. For the

dx.doi.org/10.1021/la300448y | Langmuir 2012, 28, 9174−9179

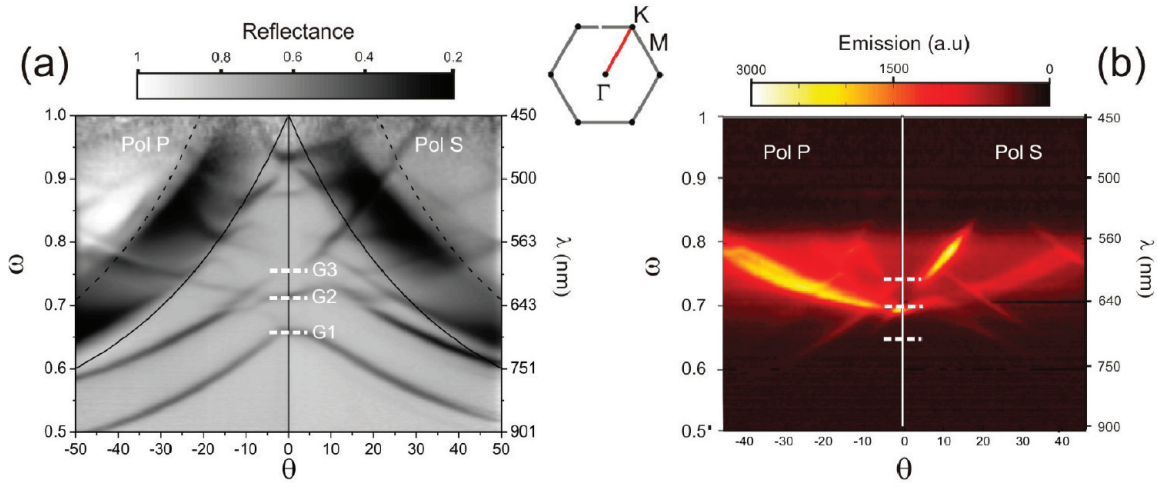

Figure 3. Angle and polarization resolved reflectance (a) and emission (b) experimental spectra for a monolayer of PS spheres with ϕ = 520 nm deposited on a silver substrate and measured along the Γ*K* direction. Inset shows the Brillouin zone of the hexagonal lattice.

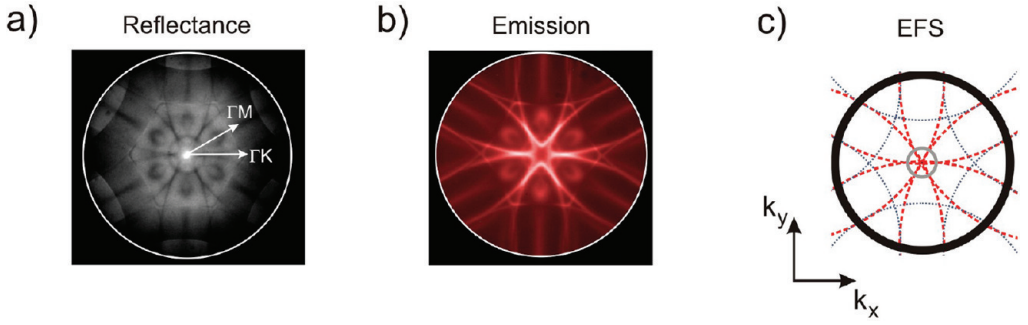

Figure 4. Experimental EFS collected in reflection (left) and emission configuration (center) for a reduced frequency ω = 0.73 (λ = 633 nm). Right panel shows a calculated EFS assuming an effective medium model with the sample parameters. Red lines correspond to a photonic mode, and the gray lines to the onset of out of plane diffraction.

imaging arm containing the CCD, no polarization selection was carried out.

RESULTS AND DISCUSSION

Angle Resolved Reflectance and PL Measurements. As a first step in the optical characterization of the samples, angle and polarization resolved reflectance measurements were collected using the above-mentioned experimental setup. In this way, the dispersion relation of the fabricated samples can be retrieved. In order to properly orient the samples so that different high symmetry directions in reciprocal space can be studied, we used the characteristic hexagonal diffraction patterns obtained with visible light. Further, when using this fabrication method, the sample retains a homogeneous hexagonal packing throughout its entire surface.[19] Figure 3a shows the dispersion relation along the ΓK direction in reciprocal space. Dark lines correspond to the different eigen modes of the system to which light from free space can couple. All the spectra are presented as a function of the normalized frequency $\omega = \sqrt{3}\phi/2\lambda$ in order to make the results scalable with the sphere diameter. Two broad dark bands appear in the diagram which corresponds to the limits where out of plane diffraction takes place while the reflected light cannot be collected by the experimental setup.[22] The spectral position of the three different modes observed at normal incidence appears highlighted with horizontal dashed lines. These correspond to modes having a marked plasmonic (G1), photonic (G2), and hybrid (G3) character, with their associated total field intensity located close to the metal surface, the sphere center or both, respectively.[6,23]

As a next step, we changed from white light to laser illumination in order to study the PL from the samples. The pump wavelength is slightly detuned from the absorption maximum of the organic dye (530 nm), but this fact did not affect our measurements. The use of a silver substrate allowed us to avoid the absorption of gold, used previously as substrate, on the optical response. For the case of silver, absorption takes place for wavelengths below the spectral range where the doped spheres emit (560−700 nm) and therefore PL measurements are not hampered by intrinsic metal losses.[23] Here we can see how the spontaneous emission of the internal sources is being channeled by those modes originating at ω = 0.7 at normal incidence (G2). These modes have a photonic character with the EM field intensity mainly localized close to the sphere center, where the organic emitter lies.[6]

Experimental Equifrequency Surfaces. So far, the optical characterization we have performed in the shape of dispersion relations gives us information on the spectral position of the modes to which light can couple and how these modes channel the emission of light sources located within the periodic dielectric array. However, as mentioned in the introduction, this information, though valuable, fails to explain how light propagates in the plane of the periodicity. EFSs represent the set of all allowed wave vectors for a given

dx.doi.org/10.1021/la300448y | *Langmuir* 2012, 28, 9174−9179

frequency and can therefore be considered as a horizontal section (that is, at a fixed frequency) of the above-discussed dispersion relations. Hence, a way to collect them with our experimental setup is to image the whole Fourier plane at once, filtering the reflected/emitted light in order to obtain a monochromatic image. The obtained image corresponds to the Fourier plane of the objective and is a circular one where each point along the radius corresponds to an angle of reflection emission, with the center corresponding to normal incidence (θ = 0°) and the edge to the NA of the objective (θ = 48°).

Figure 4a shows an EFS collected in reflection configuration for a reduced frequency ω = 0.73 (λ = 633 nm). The image presents a hexagonal symmetry, characteristic of the close packed lattice under investigation. Here we can see a set of thin dark curves over a bright background. Each of these curves corresponds to the angle at which we cross the bands in the dispersion relation of Figure 3a while moving along a fixed frequency. Therefore, each of the curves corresponds to an eigen mode of the system. Over imposed there is a broad hexagonal dark band associated with the excitation of out-of plane diffraction (dark bands in Figure 3a). The observed EFS departs from the circular shape expected for a homogeneous transparent medium[11] which derives from a quasi-linear dispersion relation. It presents a complex shape characteristic of the multiple scattering of light taking place within the sample. No gaps seem to appear in the EFS, due to the fact that the dielectric lattice we are considering presents a low refractive index contrast which prevents the opening of energy gaps in the dispersion relation.

When comparing the EFS with the angle resolved spectroscopic measurements, one must take into account that for the imaging branch of our Fourier setup we make no polarization selection, so that the EFS we observed should be compared with a superposition of the two panels in Figure 3a, corresponding to s and p polarization.

If rather than illuminating the sample with white light we pump it with a diode laser we can excite the organic dye within the spheres and collect the equivalent figure for light originating in the sample. Such a result appears in Figure 4b. Here we can see how the EFS retains its 6-fold symmetry though it presents a simpler shape, some modes becoming more evident while others becoming fainter. Again, this has its correspondence in the dispersion relation where only certain modes appear clearly visible: those channeling the spontaneous emission of the spheres. Further, for this particular frequency, we can see how the brighter part of the curves is that close to normal incidence (i.e., to the EFS center). This again has its correspondence with the dispersion relation, where for this particular reduced frequency the emission is channeled along small angles.

In order to understand the shape of the EFS, we have next modeled the optical response of the structure. Since emission is being channeled by modes having a photonic character with most of its EM field intensity located within the spheres,[6] we start by considering the EFS of an effective dielectric medium having a refractive index equal to the volume average refractive index of the monolayer (n_{eff} = 1.38). As mentioned above, such EFS is just a sphere having a radius $k = 2\pi n_{eff}/\lambda$ in k space. If we next assume a periodicity (with hexagonal symmetry) of negligible refractive index contrast, the EFS of the lattice is equivalent to consider several circular EFS centered at the different reciprocal lattice points of the array,[11] given by $\mathbf{G}_{mn} = m\mathbf{b}_1 + n\mathbf{b}_2$, where $\mathbf{b}_1$ and $\mathbf{b}_2$ are the reciprocal lattice unit vectors: $\mathbf{b}_1 = (2\pi/\phi, -2\pi/\sqrt{3}\phi)$ and $\mathbf{b}_2 = (0, 4\pi/\sqrt{3}\phi)$ and n and m integers. Introducing the experimental parameters of our study (ϕ = 520 nm, λ = 633 nm), we obtain the EFS plotted in Figure 4c. Here the red lines indicate the modes of the effective medium lattice, and the gray lines are the condition for out of plane diffraction. The coincidence of the experimental (Figure 4b) and calculated (Figure 4c) EFS is outstanding, evidencing the worth of the empty lattice approximation. Nevertheless, some differences are present, particularly close to normal incidence at the EFS center. Here the different modes of the effective medium cross each other, while in the experimental case they anticross, leaving a star shaped figure in the center of the EFS. These differences originating at anticrossings of the modes are probably the result of multiple scattering of light taking place due to the presence of an all but negligible refractive index contrast in the real structure under study in the experiment. Hence, even if the basic model we have used explains the overall shape of the experimental EFS, a more detailed model will be needed in the future in order to understand some aspects such as the exact shape of the modes or the fact that some regions of the EFS appear brighter than others, due to light emission being channeled by those modes.

Finally, we have extended the EFS study to different reduced frequencies in the range 0.64 < ω < 0.75, corresponding to the emission of the organic dye contained within the spheres. Experimental results are shown in Figure 5 for different wavelengths in the spectral range where our tunable filter operates. Note that the spectral width of the tunable filter is ±10 nm instead of the ±3 nm of the filter working at 633 nm, making the EFS in this figure less sharply defined than those in Figure 4. The sample and the optical pump conditions are identical for all measured EFS. In Figure 5, a number of things should be noted. First, the overall 6-fold shaped figures of the different EFS can be constructed as one considers circles of increasing radius in the previously described effective index model, corresponding to an increasing reduced frequency. This indicates that, at least in the spectral range under consideration, emission is always channeled by modes having a photonic character. Further, it can be appreciated that the brightest points of the EFS (i.e., the angles for which spontaneous emission is enhanced at that particular frequency) correspond to the points where circles coming from different reciprocal lattice vectors intersect. At these intersections, Bragg diffraction by several lattice vectors is taking place and one expects features such as anticrossings and gaps leading to low dispersion bands responsible for enhanced light matter interaction.[24] Though in our case the refractive index contrast is rather low and energy gaps are not present, it is enough to give rise to some band anticrossings as evident from Figure 3. Nevertheless, the exact intensity is the result of the EM mode density and the spectral shape of the light sources, and a precise description of the emission is out of the scope of this paper.

■ CONCLUSIONS

In conclusion, we have performed an ample study on how light interacts with self-assembled hybrid photonic−plasmonic crystals by means of Fourier microscopy. Such study comprises both angle resolved spectroscopic measurements, providing information on how light couples to/is emitted from the modes of the system, as well as EFS, whose shapes dictate the way light propagates in the plane of periodicity. We have considered two growth methods in order to find the structure with the highest crystalline quality allowing the former study to be carried out in the absence of spurious effects introduced by lattice disorder.

dx.doi.org/10.1021/la300448y | Langmuir 2012, 28, 9174−9179

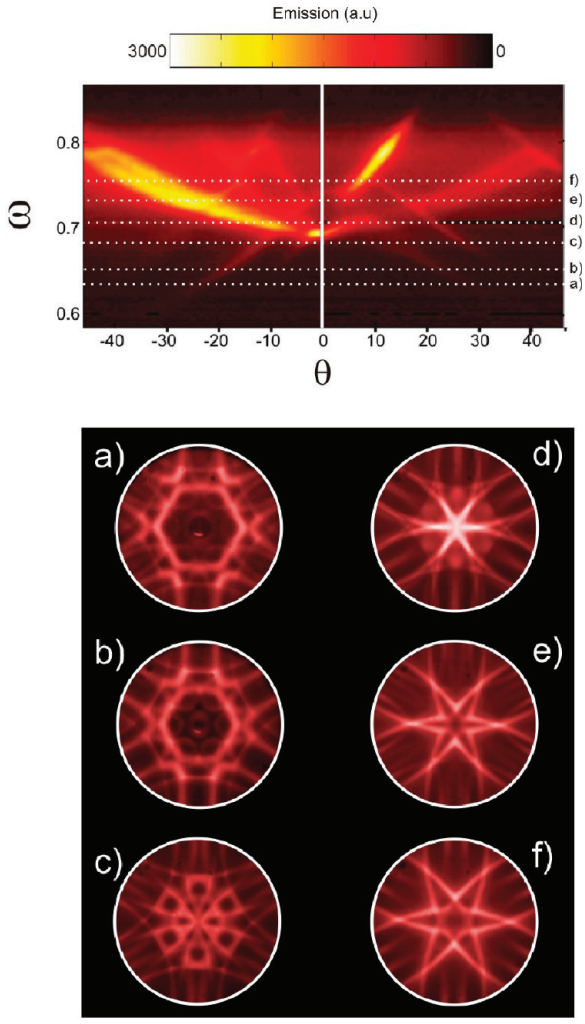

Figure 5. (Top) Angle resolved emission along the ΓK direction for p (left) and s polarized light (right). White dashed lines indicate frequencies for which EFS were collected. (Bottom) Experimental EFS for $\omega = 0.64$ (a), $\omega = 0.66$ (b), $\omega = 0.69$ (c), $\omega = 0.71$ (d), $\omega = 0.73$ (e), and $\omega = 0.75$ (f).

The obtained EFSs in both reflection and emission configuration complement spectroscopic measurements and further evidence how light emitted by organic dyes contained in the spheres forming the periodic array is channeled by modes having a photonic character. The latter is confirmed by modeling the experimental EFS with an effective medium approach which reproduces its overall shape. Discrepancies between the model and the experiment are attributed to the presence of an all but negligible refractive index contrast in the fabricated samples. Finally, we have performed a study of EFS in emission as a function of frequency which allowed us to fully characterize the complexity of the far field emission properties of these structures and could serve as a means to evaluate future applications of similar systems as efficient light sources.

AUTHOR INFORMATION

Corresponding Author

*E-mail: galisteo@icmm.csic.es (J.F.G.-L.); ablanco@icmm.csic.es (A.B.).

Notes

The authors declare no competing financial interest.

ACKNOWLEDGMENTS

M.L.-G. was supported by the FPI PhD program from the MICINN. This work was supported by the Spanish MICINN CSD2007-0046 (Nanolight.es) and MAT2009-07841 projects and Comunidad de Madrid S2009/MAT-1756 (PHAMA) programme.

REFERENCES

(1) Benson, O. Assembly of hybrid photonic architectures from nanophotonic constituents. *Nature* **2011**, *480*, 193−199.
(2) Boriskina, S. V.; Povinelli, M.; Astratov, V. N.; Zayats, A. V.; Podolskiy, V. A. Collective phenomena in photonic, plasmonic and hybrid structures. *Opt. Express* **2011**, *19*, 22024−22029.
(3) Galisteo-López, J. F.; Ibisate, M.; Sapienza, R.; Froufe-Pérez, L. S.; Blanco, A.; López, C. Self-assembled photonic structures. *Adv. Matter.* **2011**, *23*, 30−69.
(4) Romanov, S. G.; Korovin, A. V.; Regensburger, A.; Peschel, U. Hybrid colloidal plasmonic-photonic crystals. *Adv. Matter.* **2011**, *23*, 2515−2533.
(5) Shi, L.; Liu, X.; Yin, H.; Zi, J. Optical response of a flat metallic surface coated with a monolayer array of latex spheres. *Phys. Lett. A* **2010**, *374*, 1059−1062.
(6) López-García, M.; Galisteo-López, J. F.; Blanco, A.; Sánchez-Marcos, J.; López, C.; García-Martín, A. Enhancement and directionality of spontaneous emission in hybrid self-assembled photonic-plasmonic-crystals. *Small* **2010**, *6*, 1757−1761.
(7) Yu, X.; Shi, L.; Han, D.; Zi, J.; Braun, P. V. High quality factor metallodielectric hybrid plasmonic-photonic crystals. *Adv. Funct. Mater.* **2010**, *20*, 1910−1916.
(8) Grandidier, J.; Callahan, D. M.; Munday, J. N.; Atwater, H. A. Light absorption enhancement in thin-film solar cells using whispering gallery modes in dielectric nanospheres. *Adv. Mater.* **2011**, *23*, 1272−1276.
(9) Astratov, V. N.; Whittaker, D. M.; Culshaw, I. S.; Stevenson, R. M.; Skolnick, M. S.; Krauss, T. F.; De La Rue, R. M. Photonic band-structure effects in the reflectivity of periodically patterned waveguides. *Phys. Rev. B* **1999**, *60*, R16255−R16258.
(10) Kosaka, H.; Kawashima, T.; Tomita, A.; Notomi, M.; Tamamura, T.; Sato, T.; Kawakami, S. Photonic crystals for micro lightwave circuits using wavelength-dependent angular beam steering. *Appl. Phys. Lett.* **1999**, *74*, 1212−1214.
(11) Notomi, M. Theory of light propagation in strongly modulated photonic-crystals: Refractionlike behavior in the vicinity of the photonic bandgap. *Phys. Rev. B* **2000**, *62*, 10696−10705.
(12) Notomi, M.; Tamamura, T.; Ohtera, Y.; Hanaizumi, O.; Kawakami, S. Direct visualization of photonic band structure for three-dimensional photonic crystals. *Phys. Rev. B* **2000**, *61*, 7165−7169.
(13) Wierer, J. J.; David, A.; Megens, M. M. III-nitride photonic-crystal light-emitting diodes with high extraction efficiency. *Nat. Photonics* **2009**, *3*, 163−169.
(14) Schonbrun, E.; Wu, Q.; Park, W.; Yamashita, T.; Summers, C.; Abashin, M.; Fainman, Y. Wave front evolution of negatively refracted waves in a photonic crystal. *Appl. Phys. Lett.* **2007**, *90*, 041113.
(15) Le Thomas, N.; Houdré, R.; Kotlyar, M. V.; O'Brien, D.; Krauss, T. F. Exploring light propagating in photonic crystals with Fourier optics. *J. Opt. Soc. Am. B* **2007**, *24*, 2964−2971.
(16) Stein, B.; Laluet, J.-Y.; Devaux, E.; Genet, C.; Ebbesen, T. W. Surface plasmon mode steering and negative refraction. *Phys. Rev. Lett.* **2010**, *105*, 266804.
(17) Shi, L.; Yin, H.; Zhu, X.; Liu, X.; Zi, J. Direct observation of iso-frequency contour of surface modes in defective photonic crystals in real space Appl. *Phys. Lett.* **2010**, *97*, 251111.
(18) Jiang, P.; Bertone, J. F.; Hwang, K. S.; Colvin, V. L. Single-crystal colloidal multilayers of controlled thickness. *Chem. Mater.* **1999**, *11*, 2132−2140.
(19) Sun, J.; Tang, C-j.; Zhan, P.; Han, Z-l.; Cao, Z.-S.; Wang, Z.-L. Fabrication of centimeter-sized single-domain two-dimensional

colloidal crystals in a wedge-shaped cell under capillary forces. *Langmuir* **2010**, *26*, 7859−7864.
(20) Im, S.; Kim, M. H.; Park, O. Thickness control of colloidal crystals with a substrate dipped at a tilted angle into a colloidal suspension. *Chem. Mater.* **2003**, *15*, 1797−1802.
(21) Canalejas-Tejero, V.; Ibisate, M.; Golmayo, D.; Blanco, A.; López, C. Qualitative and quantitative analysis of crystallographic defects present in 2D colloidal sphere arrays. *Langmuir* **2012**, *28*, 161−167.
(22) López-García, M.; Galisteo-López, J. F.; López, C. Angle and polarization resolved optical characterization of photonic structures through Fourier imaging spectroscopy. Submitted for publication, 2012.
(23) Galisteo-López, J. F.; López-García, M.; López, C.; García-Martín, A. Intrinsic losses in self-assembled hybrid metallodielectrc systems. *Appl. Phys. Lett.* **2011**, *99*, 083302.
(24) Krauss, T. F. Slow light in photonic crystal waveguides. *J. Phys. D: Appl. Phys* **2007**, *40*, 2666−2670.